Supplementary Material (ESI) for Journal of Materials Chemistry


# Electronic Supplementary Information (ESI) for "Designer Electrode Interfaces: Diffusional Protection of Electrodes Using Chemical Architectures" Experimental Techniques Numerical Simulations

*Gregory G. Wildgoose, François G. Chevallier, Lei Xiao, Charles A. Thorogood, Shelley J. Wilkins, Alison Crossley, Li Jiang, Timothy T. G. Jones, John H. Jones, Richard G. Compton*[*]

## 1. Experimental

### 1.1 Reagents and equipment

All reagents were purchased from Aldrich (Gillingham, UK) with the exception of the glassy carbon microspheres (10-20 μm diameter, Type I) which were purchased from Alfa Aesar (Karlsruhe, Germany) and were of the highest commercially available grade. All aqueous solutions were prepared using deionised water with a resistivity not less than 18.2 MΩ cm at $25^0$C (Vivendi Water Systems, UK)

Electrochemical measurements were performed using a μAutolab potentiostat (Ecochemie, Netherlands) controlled by a PC. A three electrode cell set-up was used throughout consisting of either a gold (1mm diameter, GoodFellow, Cambridge, UK) or eppg (diameter = 4mm, LeCarbone, Sussex, UK) working electrode (see text), a platinum coil (99.99%, GoodFellow, Cambridge, UK) counter electrode and a saturated calomel electrode (SCE, Radiometer, Copenhagen, Denmark) as the reference electrode. LSASV analysis was performed using solutions of either sodium meta arsenite in 0.1 M HCl or copper(II) nitrate in 0.1 M $H_3PO_4$ using a deposition potential of -0.3 V or -1.5 V vs. SCE respectively for deposition times ranging from 10-90 s (see text). The potential was then scanned at 75 $mVs^{-1}$ over the potential region of interest. The cell was degassed with pure nitrogen (BOC, Guildford, Surrey, UK) for 20 minutes prior to any electrochemical experiment being performed.
Scanning electron microscopy (FEG-SEM) was performed using a JEOL 6500F instrument.

[*] Corresponding author. Email: richard.compton@chem.ox.ac.uk

## 1.2 Modification of glassy carbon microspheres with L-cysteine methyl ester:

The procedure for modifying glassy carbon spheres with L-cysteine methyl ester (CysOMe) has been published elsewhere[1] but briefly involves the following protocol:

2g of glassy carbon microspheres (10-20 μm diameter, GC) was stirred at room temperature with 10 $cm^3$ of thionyl chloride ($SOCl_2$) for 1 hour in order to convert the carboxyl groups, known to be present on the surface of glassy carbon to the corresponding acyl chloride moieties (GC-COCl). The resulting GC-COCl was then washed with dry chloroform to remove any thionyl chloride and other impurities from the powder. Next the GC-COCl powder was suspended in 10 $cm^3$ of dry chloroform containing 0.5g of CysOMe.HCl and 0.27 $cm^3$ of dry triethylamine ($Et_3N$) was slowly added. The reaction mixture was then stirred under argon for 12 hours at room temperature. After which time the CysOMe modified GC powder (CysOMe-GC) was washed with copious quantities of chloroform, dichloromethane, acetonitrile and pure water to remove any unreacted species from the CysOMe-GC powder. The protocol is shown schematically in scheme 1.

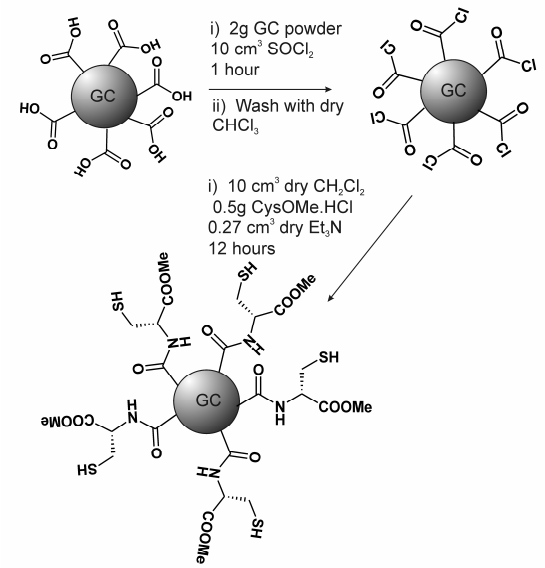


**Scheme 1:** The covalent modification of glassy carbon microspheres with L-cysteine methyl ester.

## 1.3 Modification of an edge-plane pyrolytic graphite electrode (eppg) with a monolayer of CysOMe-GC microspheres

First the eppg working electrode was polished using 1μm and 0.3 μm alumina with sonication between each polishing to remove any alumina microparticles. Next the eppg electrode surface was oxidised using cyclic voltammetry in 0.1 M $HNO_3$. Five cycles were performed scanning between 0.0 to +2.0 V vs. SCE. This procedure oxidises oxygen-containing surface functional groups, such as hydroxyl and quinonyl moieties, which are known to decorate the edge-plane sites on graphite surfaces, to the corresponding carboxyl groups.[2] The oxidised eppg electrode was then suspended

in thionyl chloride (ca. 20 $cm^3$) and stirred for one hour, to convert the surface carboxyl groups to acyl chloride moieties (eppg-COCl).

After this time the eppg-COCl electrode was removed from the thionyl chloride under a nitrogen atmosphere to prevent any atmospheric hydrolysis of the acyl chloride groups. The electrode was inverted and heat shrink tubing was fitted tightly around the end of the electrode as shown in scheme 2. The heat shrink tubing "cup" was then filled with 2 $cm^3$ of a suspension of CysOMe-GC in dry chloroform (2mg CysOMe-GC / $cm^3$ of chloroform) to which 5 drops of triethylamine (excess) was added slowly. The electrode was then left overnight. Finally the modified eppg electrode was washed with acetonitrile and pure water and sonicated briefly for 3 s to remove any unattached microspheres. The sonication process ensures that only those CysOMe-GC microspheres that are strongly covalently anchored onto the eppg electrode surface remain to produce a monolayer of CysOMe-GC spheres protecting the eppg electrode surface as shown in figure 1b in the paper. The covalent attachment of the CysOMe-GC spheres is believed to occur through the free thiol group in the CysOMe molecule to form xanthate ester linkages to the eppg surface, shown in scheme 3.

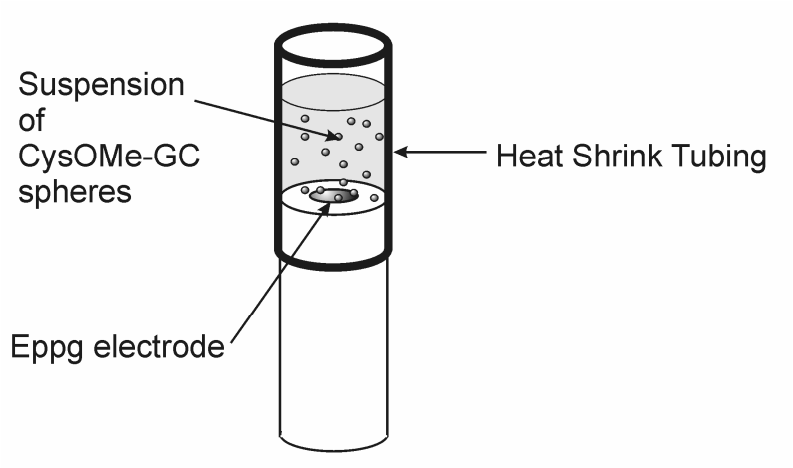


**Scheme 2:** showing how the CysOMe-GC spheres were allowed to react with the eppg-COCl electrode

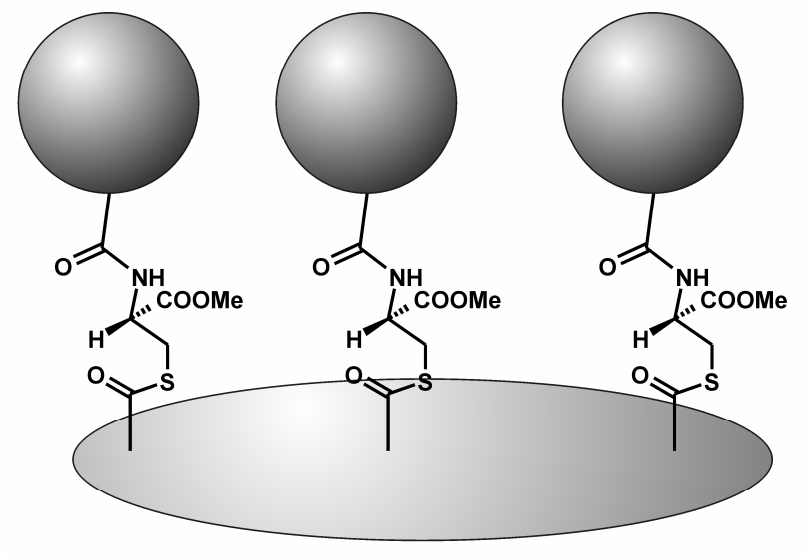


**Scheme 3:** showing the covalent attachment of the CysOMe-GC microspheres onto the eppg electrode to form a monolayer CysOMe-GC protected eppg electrode

### 1.4 Modification of an edge-plane pyrolytic graphite electrode (eppg) with a multilayer of CysOMe-GC microspheres

First a CysOMe-GC protected eppg was prepared as above and was surrounded by a heat shrink tubing "cup" again as described above. GC spheres which had been treated with thionyl chloride to form GC-COCl microspheres were then suspended in a dry solution of chloroform (2mg GC-COCl / $cm^3$ chloroform) and $2cm^3$ of this suspension was added into the heat shrink tubing "cup" along with a few drops of triethylamine. The electrode was then left overnight under a nitrogen atmosphere to prevent any unwanted hydrolysis of the unreacted acyl chloride groups on the GC-COCl surface. Again, microspheres that were not covalently attached were removed by sonication as described above. This then produces a monolayer of CysOMe-GC spheres covalently attached to the eppg electrode with a covalently attached layer of GC-COCl modified spheres above that. By repeating the process and alternating between the addition of CysOMe-GC and GC-COCl spheres successive multilayers of modified microspheres can be built up in a relatively controlled fashion as shown schematically in scheme 4 and in figure 1b in the paper.

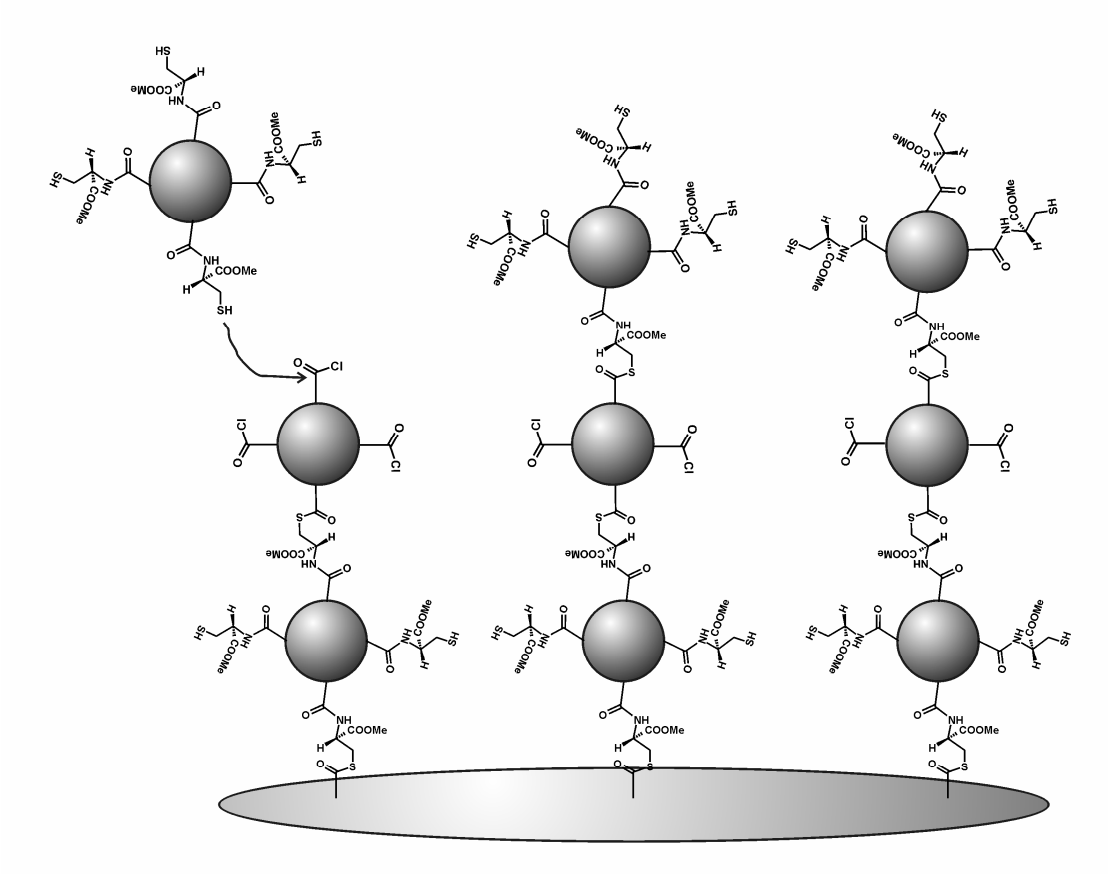

**Scheme 4:** The building up of multilayers of modified GC microspheres on an eppg electrode.

## 1.5 Modification of a gold macrodisc electrode with a sparse monolayer of CysOMe-GC spheres

Casting solutions of CysOMe-GC microspheres suspended in water were made up with the following ratios: 0.1 mg / $cm^3$ of water; 1mg / $cm^3$ of water; 3mg / $cm^3$ of water. A 2µL aliquot of the appropriate casting solution was then placed over the electrode surface and the solvent was allowed to slowly evaporate by placing the electrode in an oven at 40 $^0$C. The modified electrode was checked using an optical microscope equipped with a digital camera before and after use and no

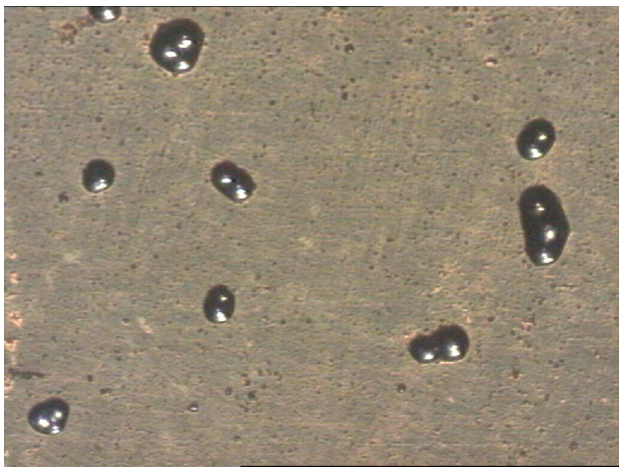

***Supplementary figure 1:*** A sparse monolayer of CysOMe-GC microspheres

appreciable loss of microspheres was observed during the experiment. As can be seen in supplementary figure 1 the coverage of CysOMe-GC microspheres forms a sparse monolayer.

## 2. Mathematical modeling and numerical simulation using the diffusion domain approach

The interface was modelled by considering a planar electrode of surface area $A_{elec}$ covered with $N$ randomly dispersed spherical microparticles of radius $r_p$. The phenomenon of interest is the competition taking place between two distinct physical processes: the electrodeposition of species $A$ onto the electrode surface and the adsorption of the same species on the microparticles' surface. For the sake of simplicity we ignore the volume of the particles; instead approximate them by flat disks of radius $r_p$ characterised by a maximum surface concentration $\Gamma_{pi}$ and a time/position dependent concentration $\Gamma_p$ (Supplementary Figure 2). The process of adsorption onto the surface of both the particles and the electrode is then modelled by an irreversible Langmuirian adsorption reaction. This allows the quantity of material deposited onto the electrode surface at any time to be measured. However, to capture the main features of electrodeposition the adsorption parameters (rate constant and maximum surface concentration) at the electrode surface are assigned values in such a way that the electrode surface never 'fills up' completely and that the adsorption step is never the limiting process. These hypotheses allow us to simplify the model, so that it is mathematically tractable, while remaining realistic enough for the analysis to be meaningful.

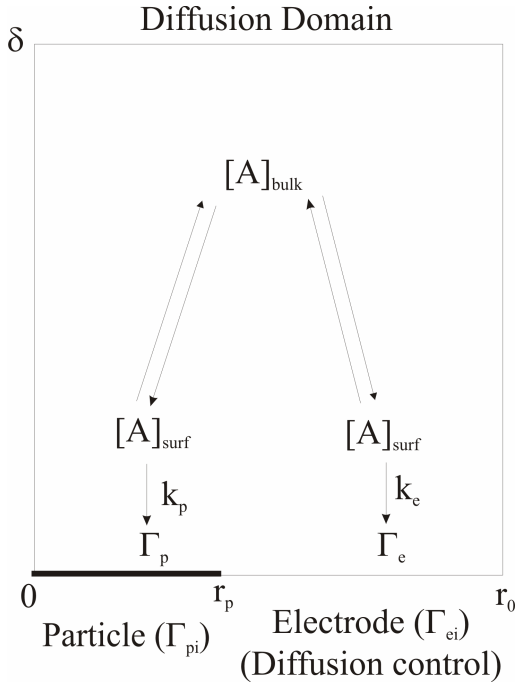


***Supplementary Figure 2.*** Schematic of the electrodeposition reaction in the presence of microparticles.

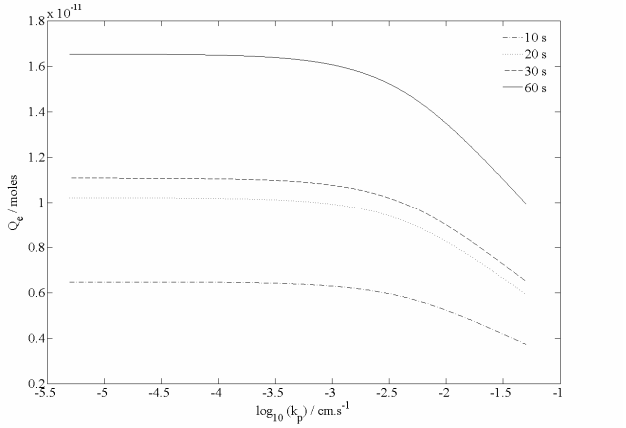


***Supplementary Figure 3.*** Simulated variation of $Q_e$ as a function of $\log_{10}(k_p)$. The parameters used for simulation are as follows: $[A]_{bulk} = 2x10^{-8}$ mol cm$^{-3}$, $r_p = 6x10^{-4}$ cm, $D_{As} = 1.2x10^{-5}$ cm$^2$ s$^{-1}$, $\Gamma_{pi} = 7.1x10^{-10}$ mol cm$^{-2}$, $\Gamma_{ei} = 1$ mol cm$^{-2}$, $k_e = 5x10^6$ cm s$^{-1}$, $\Theta$=0.087, $A_{elec}$=5.578x10$^{-3}$ cm$^2$.

The particles are assumed to be randomly distributed over the electrode surface, therefore the response of the electrode is modelled using the diffusion domain approximation, which has been presented in detail in previous publications[3, 4] and will therefore not be described here. The response of the system is given by the sum of the responses of individual diffusion domains of radius $r_0$. This generic approach has already been used for various systems and has been shown to be computationally very

efficient whilst retaining physical accuracy.[3-9] Under the conditions stated above, we can define the global coverage of the electrode, $\Theta$, as:

$$\Theta = \frac{N\pi r_p^2}{A_{elec}} \quad (0.1).$$

The modelling was performed using experimentally determined parameters to generate working curves representing the quantity of material deposited onto the electrode surface, $Q_e$, as a function of the particle adsorption rate constant $k_p$ (Supplementary Figure 3).

The following reaction is taking place at the electrode surface:

$$A^{n+} + ne^- \xrightarrow{k_e} A(s) \qquad (2)$$

while at the particles' surface we have the following process.

$$A \xrightarrow{k_p} A_{ads} \qquad (3)$$

Both the adsorption onto the particle and the electrodeposition reaction are modelled by an irreversible Langmuirian adsorption isotherm. Therefore both the particle and the electrode surface are characterized by a maximum surface concentration expressed in mol cm$^{-2}$ ($\Gamma_{pi}$ and $\Gamma_{ei}$ for the particle and the electrode respectively) and an adsorption rate constant with units cm s$^{-1}$ ($k_p$ for the particle and $k_e$ for the electrode). In order to model the electrodeposition reaction correctly, $\Gamma_{ei}$ and $k_{ei}$ are assigned very high values such that the maximum surface concentration is never reached and that the electrodeposition step is always controlled by diffusion. The system presented in the Supplementary Figure 2 requires the modelling of different processes: diffusion of species $A$ in the bulk of the solution, deposition of $A$ onto the electrode surface and, competitively, adsorption of $A$ on the electrode surface. As a consequence, the mathematical model is composed of three distinct partial differential equations corresponding to the different processes:

$$\frac{\partial[A]}{\partial t} = D_A\left(\frac{\partial^2[A]}{\partial r^2} + \frac{1}{r}\frac{\partial[A]}{\partial r} + \frac{\partial^2[A]}{\partial z^2}\right) \qquad (4)$$

$$\Gamma_{ei}\frac{\partial\Gamma_e}{\partial t} = k_e(\Gamma_{ei} - \Gamma_e)[A]_{surf} \qquad (5)$$

$$\Gamma_{pi}\frac{\partial\Gamma_p}{\partial t} = k_p(\Gamma_{pi} - \Gamma_p)[A]_{surf} \qquad (6)$$

equation (4) describes the mass transport of $A$ in the cylindrical coordinate system,[3, 4] while equations (5) and (6) corresponds to the evolution of the surface concentration on the electrode and the particle respectively. The symbols $D_A$ and [$A$] represent the diffusion coefficient / $cm^2\ s^{-1}$ and the concentration / mol $cm^{-3}$ of species $A$ in the bulk of the solution.

At the beginning of the electrochemical experiment only species $A$ is present in the solution. Therefore the initial conditions ($t = 0$) for the concentrations of the species taking part in the reaction are:

| | | | | | |
|---|---|---|---|---|---|
| $[A] = [A]_{bulk}$ | for | $0 \le r \le r_0$ | and | $0 \le z < \infty$ | |
| $\Gamma_p = 0$ | for | $0 \le r < r_p$ | and | $z=0$ | |
| $\Gamma_e = 0$ | for | $r_p \le r < r_0$ | and | $z=0$ | (7) |

the geometry of the simulation space implies a concentration equal to $[A]_{bulk}$ at the semi-infinite boundary as well as a non-flux boundary condition on the symmetry axis and the diffusion domain wall. These conditions are translated mathematically as in the table below

| | | | | | |
|---|---|---|---|---|---|
| $[A] = [A]_{bulk}$ | for | $0 \le r \le r_0$ | and | $z \to \infty$ | |
| $\frac{\partial[A]}{\partial r} = 0$ | for | r =0 | and | $0 \le z < \infty$ | |
| $\frac{\partial[A]}{\partial r} = 0$ | for | r = $r_0$ | and | $0 \le z < \infty$ | (8) |

At the electrode surface we have the following condition:

$$D_A \frac{\partial [A]}{\partial z} = k_e \left(\frac{\Gamma_{ei} - \Gamma_e}{\Gamma_{ei}}\right)[A]_{surf} \qquad \text{for} \qquad r_p \le r < r_0 \qquad \text{and} \qquad z = 0 \qquad (9)$$

while at the particle surface we have:

$$D_A \frac{\partial [A]}{\partial z} = k_p \left(\frac{\Gamma_{pi} - \Gamma_p}{\Gamma_{pi}}\right)[A]_{surf} \qquad \text{for} \qquad 0 \le r < r_p \qquad \text{and} \qquad z = 0 \qquad (10)$$

Since both the electrode and the particle surface concentrations are not only a function of time but also a function of position, the interpretation of the results can be simplified by introducing average surface concentrations, defined as:

$$\overline{\Gamma}_p = \frac{2}{r_p^2}\int_0^{r_p} \Gamma_p \, r \, dr$$

$$\overline{\Gamma}_e = \frac{2}{r_0^2 - r_p^2}\int_{r_p}^{r_0} \Gamma_e r \, dr \qquad (11)$$

therefore, for a single diffusion domain, at any time, the amounts of *A* taken up by the electrode surface, $Q_e$, and the particle surface, $Q_p$, can be calculated using equation(12).

$$Q_e = \overline{\Gamma}_e \times \pi\left(r_0^2 - r_p^2\right)$$

$$Q_p = \overline{\Gamma}_p \times \pi r_p^2 \qquad (12)$$

Summation of the individual responses of all the diffusion domains present on the electrode surface allows determination of the total uptake of *A* by the particles and the electrode surface.

## 2.1 Computation

A fully implicit discretization scheme[5] combined with Newton's method[5] and a modified version of the Thomas algorithm[6] was used to solve the system of partial

differential equations. The simulation space was covered with an expanding grid similar to the one presented in previous publications[7-9] and which will therefore not be described here. The simulation program was tested for both spatial and temporal convergence to ensure that the solution satisfies the accuracy requirement for the quantity of interest[3, 4] (less than 1% variation from the asymptotic average surface concentration value for all scan rates considered). All the programs for the simulations were written in Delphi 7© and executed on a PC with Pentium 4 2.5 GHz processor and 1 GB of RAM. The convergence and accuracy of the simulation program were tested in the same way as described in previous publications.[3, 4]

**2.3 Theory *vs.* experiments**

Numerical simulation was used to determine an average value for the adsorption rate constant of $A$ onto the particles surface for different deposition times. All the parameters required by the simulation code were determined using experimental results. Once all the parameters were known, the code was set up to generate working curves representing the quantity of material deposited onto the electrode surface as a function of the particle adsorption rate constant $k_p$. The results are shown in figure 3 in the Communication, where it can be seen that, as the value of $k_p$ decreases, the amount of material deposited on the electrode surface, $Q_e$ , increases up to a point where the curve exhibit a plateau. This plateau corresponds to a limit where the value of $k_p$ is such that the presence of the microparticles is negligible. Although this phenomenon is seen for all deposition times considered, closer observation of Supplementary figure 3 shows that the transition between the region where the particles affect the system and the region where the plateau occurs is dependent on the deposition time. This is probably due to the fact that if the

deposition time considered is short then the effects of mass transport are less perceptible. Also, since the electrodeposition process occurs at a greater rate than the adsorption process, the effects of the latter are negligible unless the value of $k_p$ is sufficiently high.

Once the working curves have been simulated, it is possible to use them to determine an average value for the adsorption rate constant of the experimental system under consideration. Using the LSASV voltammetry it was possible to determine $Q_e$ for each deposition time; using these values and the corresponding working curve, we can then determine the value of $k_p$ via interpolation. The results obtained are shown in the table below.

| Deposition time / s | $k_p$ / cm $s^{-1}$ |
|---|---|
| 10 | $9.35 \times 10^{-4}$ |
| 20 | $6.97 \times 10^{-4}$ |
| 30 | $5.79 \times 10^{-4}$ |
| 60 | $2.74 \times 10^{-4}$ |

The variation of $k_p$ with deposition time reflects the average rate constant's dependence on the surface concentration of available adsorption sites, which decreases over time.

## 3. References

1 G. G. Wildgoose, H. C. Leventis, A. O. Simm, J. H. Jones, R. G. Compton, *Chem. Commun.*, 2005, 3694

2 R. L. McCreery in *Electroanalytical Chenmistry*, ed. A. J.\ Bard, Marcel Dekker, New York, 1990, Vol 17, pp. 221

3 F. G. Chevallier, T. J. Davies, O. V. Klymenko, L. Jiang, T. G. J. Jones, R. G. Compton, *J. Electroanal. Chem.*, 2005, **580**, 265

4 F. G. Chevallier, T. J. Davies, O. V. Klymenko, L. Jiang, T. G. J. Jones, R. G. Compton, *J. Electroanal. Chem.*, 2005, **577**, 211

5 K. Eriksson, D. Estep, P. Hansbo, C. Johnson in *Computational Differential Equations*, Cambridge University Press, Cambridge, UK, 1996

6 I. Svir, O. V. Klymenko, R,. G. Compton, *Radiotekhnika*, 2001, **118**, 92

7 B. A. Brookes, T. J. Davies, A. C. Fisher, R. G. Evans, S. J. Wilkins, K. Yunus, J. D. Wadhawan, R. G. Compton, *J. Phys. Chem. B*, 2003, **107**, 1616

8 T. J. Davies, B. A. Brookes, A. C. Fisher, K. Yunus, S. J. Wilkins, P. R. Greene, J. D. Wadhawan, R. G. Compton, *J. Phys. Chem. B*, 2003, **107**, 6431

9 T. J. Davies, B. A. Brookes, R. G. Compton, *J. Electroanal. Chem.*, 2004, **566**, 193